



**HAL**  
open science

## Non-equilibrium charge density wave ground state of quasi-two-dimensional rare-earth tritelluride TbTe 3

A V Frolov, A P Orlov, D M Voropaev, A. Hadj-Azzem, A A Sinchenko, P. Monceau

► **To cite this version:**

A V Frolov, A P Orlov, D M Voropaev, A. Hadj-Azzem, A A Sinchenko, et al.. Non-equilibrium charge density wave ground state of quasi-two-dimensional rare-earth tritelluride TbTe 3. Applied Physics Letters, 2023, 118 (25), pp.253102. 10.1063/5.0051588 . hal-03964636

**HAL Id: hal-03964636**

**<https://hal.science/hal-03964636>**

Submitted on 31 Jan 2023

**HAL** is a multi-disciplinary open access archive for the deposit and dissemination of scientific research documents, whether they are published or not. The documents may come from teaching and research institutions in France or abroad, or from public or private research centers.

L'archive ouverte pluridisciplinaire **HAL**, est destinée au dépôt et à la diffusion de documents scientifiques de niveau recherche, publiés ou non, émanant des établissements d'enseignement et de recherche français ou étrangers, des laboratoires publics ou privés.



# Non-equilibrium charge density wave ground state of quasi-two-dimensional rare-earth tritelluride $\text{TbTe}_3$

Cite as: Appl. Phys. Lett. **118**, 253102 (2021); doi: 10.1063/5.0051588

Submitted: 26 March 2021 · Accepted: 4 June 2021 ·

Published Online: 21 June 2021



View Online



Export Citation



CrossMark

A. V. Frolov,<sup>1</sup>  A. P. Orlov,<sup>1,2</sup>  D. M. Voropaev,<sup>3</sup> A. Hadj-Azzem,<sup>4</sup> A. A. Sinchenko,<sup>1,5,a)</sup>  and P. Monceau<sup>4</sup>

## AFFILIATIONS

<sup>1</sup>Kotelnikov Institute of Radioengineering and Electronics of RAS, 125009 Moscow, Russia

<sup>2</sup>Institute of Nanotechnology of Microelectronics of RAS, 115487 Moscow, Russia

<sup>3</sup>Moscow Institute of Physics and Technology (State University), 141701 Dolgoprudny, Moscow Region, Russia

<sup>4</sup>Université Grenoble Alpes, CNRS, Grenoble INP, Institut Néel, 38000 Grenoble, France

<sup>5</sup>M.V. Lomonosov Moscow State University, 119991 Moscow, Russia

**Note:** This paper is part of the APL Special Collection on Charge-Density-Wave Quantum Materials and Devices.

<sup>a)</sup>Author to whom correspondence should be addressed: [aaasinch@mail.ru](mailto:aaasinch@mail.ru)

## ABSTRACT

We have studied the time dependence of the relaxation of the non-equilibrium charge density wave (CDW) toward an equilibrium ground state in  $\text{TbTe}_3$  when the sample is cooled through the Peierls transition temperature under an electric field down to a given temperature,  $T_{\text{exp}}$ . We show that when cooled at zero electric field or a value less than the threshold one,  $E_b$ , for depinning the CDW at  $T_{\text{exp}}$ , the CDW equilibrium ground state has a single phase in the sample volume. When cooled with an electric field higher than  $E_b$ , the CDW ground state is in a frozen glass state, which can be destabilized only by reducing the electric field below  $E_b$ . We tentatively interpret these results by the interaction of the CDW with a well ordered Te–Te discommensuration network.

Published under an exclusive license by AIP Publishing. <https://doi.org/10.1063/5.0051588>

The Peierls instability that appears in some low-dimensional systems in decreasing temperature<sup>1,2</sup> is characterized by the opening of an energy gap at the Fermi level,  $E_F$ , resulting from the periodic lattice distortion at  $Q = 2k_F$  and a modulation of the electronic charge density with the same periodicity. The CDW order parameter is defined as  $\Delta \propto \exp(iQr + \phi)$ , where  $\phi$  is the CDW phase with respect to the lattice. For an ideal pure system, following Fröhlich,<sup>3</sup>  $\phi$  is independent of the position, which implies dissipationless charge transfer. In a real system,  $\phi$  is pinned and the sliding of CDW occurs only above a threshold value of an applied electric field. The CDW ground state results from the competition between elastic deformations of the CDW and pinning potentials provided by randomly distributed impurities, defects, interchain interactions, commensurability, and others. Therefore, in the pinning state due to disorder, the CDW has many metastable states characterized by local deformations in the CDW phase inducing an average macroscopic polarization. The randomness of the pinning centers yields a possible relation between glassy systems and CDWs.<sup>4</sup> Thus, the signature of the CDW low energy excitations (LEE) was revealed by their contribution to the specific heat in addition to that of phonons at very low temperature.<sup>5</sup>

Rearrangement of pinned CDW configurations can also be provided by dielectric relaxation in the pinned state.<sup>6</sup> Relaxation of the polarization deviates from the simple exponential decay that reflects disorder effects from impurities with a distribution of relaxation times due to a wide scale of metastable pinned configurations.

Recently, another kind of a CDW glassy-like behavior has been observed in the quasi-two dimensional compound  $\text{TbTe}_3$ .<sup>7,8</sup> In this compound, the unidirectional incommensurate CDW with  $T_{CDW} = (310\text{--}340)$  K develops along the  $c$ -axis with the wave vector  $\mathbf{Q}_{CDW1} = (0, 0, 0.296)$ . When cooled at the rate of a few degree/min (typical rate for cooling) through the Peierls phase transition, the CDW ground state of the  $\text{TbTe}_3$  is not at the equilibrium, but time dependent. That is reflected by the increase in the threshold electric field for depinning the CDW and initiation of the sliding for samples that were exposed a long time at a fixed  $T_{\text{exp}} < T_{CDW1}$ . At all exposition temperatures, the threshold electric field demonstrates an exponential dependence on time ( $E_0 - E_t(t) \sim (1 - \exp(t/\tau))$ ), where  $E_0$  is the saturating threshold field at which  $E_t$  tends under long time exposition. The characteristic time constant,  $\tau$ , for such a process is strongly temperature dependent and varies from 40 min at  $T = 320$  K

up to  $10^3$  min at  $T = 260$  K. The temperature dependence of  $E_t$  for such type exposed samples is nonmonotonic, demonstrating a large maximum at  $T = T_{\text{exp}}$ . The resistance in the CDW static state does not change with time evolution at any  $T_{\text{exp}}$ , indicating that all the changes take place in the CDW subsystem. This phenomenon was not observed before for quasi-one-dimensional CDWs and appears to be specific to the two-dimensional nature of the RTe<sub>3</sub> compounds.

The temperature dependence of  $E_t$  for exposed TbTe<sub>3</sub> single crystals shares some analogy with the dependence of the critical current in superconductors, known as the peak effect.<sup>9</sup> The explanation of this effect is based on the concept of the melting of the Abrikosov vortex lattice and the corresponding change of the pinning regime from weak collective to strong individual pinning centers.<sup>9,10</sup> Both the threshold field in the charge density wave and the critical current in superconductors are determined by pinning. By analogy with the peak effect in superconductors, a similar mechanism may be expected also for TbTe<sub>3</sub> samples. In this scenario, the observed sharp maximum of  $E_t(T)$  would be due to the melting of some defect structure of the CDW. However, the nature of these defect structures is still unclear.

In the present paper, we have studied the time dependence of the threshold electric field (the probe for the evolution of the CDW ground state) at a given  $T_{\text{exp}}$  when the samples are cooled from the  $T > T_{CDW1}$  in two configurations: first, with zero electric field (ZEFC) as in our previous work<sup>8</sup> and second, with application of an electric field (EFC). We show that in the EFC regime with the applied current higher than the value for sliding at  $T = T_{\text{exp}}$ , the time evolution of  $E_t$  is suppressed. We have also studied the Shapiro step structures in these two configurations.

Single crystals of TbTe<sub>3</sub> were grown in a pure argon atmosphere by the technique described in our previous work.<sup>11</sup> Thin rectangular single-crystal samples thinner than  $1 \mu\text{m}$  were prepared by micromechanical exfoliation of relatively thick crystals preliminarily glued on a sapphire substrate by Stycast 1266. The thickness of glue was very small, typically less than  $100 \text{ nm}$ . The quality of crystals and the spatial position of crystallographic axes were monitored by x-ray diffraction. Bar structures were prepared by etching with the use of a focused ion beam. Electrical contacts were prepared by gold evaporation and cold soldering of In. A typical contact resistance was less than  $1 \Omega$ . Hereafter, we report results obtained on two of these bar structures: structure 1 with dimensions (length among potential probes, width, and thickness)  $70 \times 13 \times 0.10$  and structure 2 with dimensions  $145 \times 35 \times 0.12 \mu\text{m}$ . The SEM image of structure 1 is shown in Fig. 1(a). Resistances, current-voltage characteristics (IVc), and their derivatives,  $dV/dI$ , of these structures were measured by the four-probe method in the current mode with a Keithley 2400 current source and a Keysight 34420A nanovoltmeter. The duration of single IV curve measurement was 28 s. The prepared structures were either ZEFC or EFC cooled from  $T > T_{CDW1}$  down to a given temperature  $T_{\text{exp}}$  below  $T_{CDW1}$  in the range 220–330 K. Temperature dependencies of resistance,  $R(T)$ , are shown in both regimes for structure 1 in Fig. 1(b). After stabilization of the temperature, time evolution of IVc was measured automatically with a fixed time interval, typically 30 min, during several tens of hours. For some samples, the IVc measurements were performed under joint application of an rf electric field with a frequency 10–40 MHz and dc electric field for Shapiro steps measurements. Before each exposition, the sample was warmed above  $T_{CDW1}$ .

A three dimensional plot illustrating results of measurements in structure 1 is shown in Fig. 1 for exposition at  $T_{\text{exp}} = 270$  K during 15 h. In Figs. 1(c), 1(e), and 1(g), we show the evolution of differential IVc with time at currents  $I_{\text{exp}} = 0, 0.3,$  and  $1.4$  mA correspondingly. Figures 1(d), 1(f), and 1(h) represent initial ( $t = 0$ ) and final ( $t = 15$  h) dependencies  $dV/dI(V)$  with subtraction of Joule heating as it was done in Ref. 8 for the corresponding  $I_{\text{exp}}$  indicated by green lines in the plots. Transition to the CDW sliding state is manifested as a very sharp decrease in differential resistance at threshold voltage  $V_t$ . In the tritelluride compounds, this change of resistance is small and amounts typically 3%–5% from the total resistance, indicating a very low velocity of the CDW motion.<sup>11,12</sup> The threshold current for sliding in structure 1 is  $I_t = 0.38$  mA at  $T = 270$  K at  $t = 0$ . So, Fig. 1(c) represents time evolution of IVc in the static CDW state during the exposition at  $I_{\text{exp}} = 0$  (ZEFC), (e) and (g) in the EFC configuration; (e)—at current  $I_{\text{exp}} = 0.3$  mA less than  $I_t$  when the CDW is still in the static state and (g)—at  $I_{\text{exp}} = 1.4$  mA in the sliding CDW state. Panels (d), (f), and (h) show corresponding differential IVc before (black curves) and after (red curves) exposition of the structure during 15 h.

As can be seen, the observed evolution of the threshold voltage under exposition at zero current is nearly the same as it was reported in Ref. 8:  $V_t$  rapidly increases at short time and demonstrates a tendency to saturation at longer time. After exposition during 15 h,  $V_t$  has increased near four times. The same behavior is observed for exposition current  $I_{\text{exp}} = 0.3$  mA, indicating that in the absence of the CDW sliding, the quasiparticle current of non-condensed carriers does not affect the time evolution of the threshold voltage. It is worth noting that at long time of exposition  $dV/dI$  exhibits a very sharp negative jump at the threshold voltage in contrast to initial time ( $t = 0$ ). Actually, a different picture is observed in the case of exposition current larger than  $I_t$ . As can be seen in Figs. 1(g) and 1(h), there is no increase in  $V_t$  during all the time of exposition.

In Figs. 2(a) and 2(c) is plotted the time evolution of IVs at  $T = 280$  K for structure 2 in the EFC regime with  $I_{\text{exp}} = 3.5$  larger than  $I_t = 0.7$  mA for this structure from  $t = 0$  [point A in Fig. 2(a)] to  $t = 22$  h [point B in Fig. 2(a)]. Similarly to the results shown in Figs. 1(g) and 1(h), there is no change in the IVs. At point B,  $I_{\text{exp}}$  is reduced to  $I_{\text{exp}} = 0.5$  mA  $< I_t$  and time evolution is followed up to 48 h [point C in Fig. 2(a)]. The increase in  $E_t$  is resumed similarly to the data for structure 1 as shown in Figs. 1(c) and 1(d). Figures 2(b) and 2(d) show results for an inverse procedure: first, the structure is EFC cooled with  $I_{\text{exp}} = 0.5$  mA  $< I_t$  and time evolution of IVs is followed 48 h from point D to point E in Fig. 2(b). Then the exposition current was sharply increased up to  $I_{\text{exp}} = 3.5$  mA  $> I_t$ . As seen in Fig. 2(b), there is a small but sharp decrease in the threshold voltage just in the vicinity of point E and no more evolution in the IVs during further exposition time up to 72 h. Panels (c) and (d) demonstrate differential current–voltage characteristics with subtraction of Joule heating as it was done in Ref. 8 at points A (red), B (green), and C (blue) for processes, which is shown in Fig. 2(a) and for points D (red), E (green), and F (blue) for processes, which is shown in Fig. 2(b). Solid pink lines indicate positions of currents 0.5 and 3.5 mA in the curves.

The fingerprint of the CDW sliding is low-frequency broadband electric noise (BBN) and narrowband noise (NBN) generation.<sup>1,2</sup> The collective electronic transport and the NBN generation can be characterized in terms of the CDW coherence and homogeneity of the CDW in space and time. The coherence can be stimulated by external radio

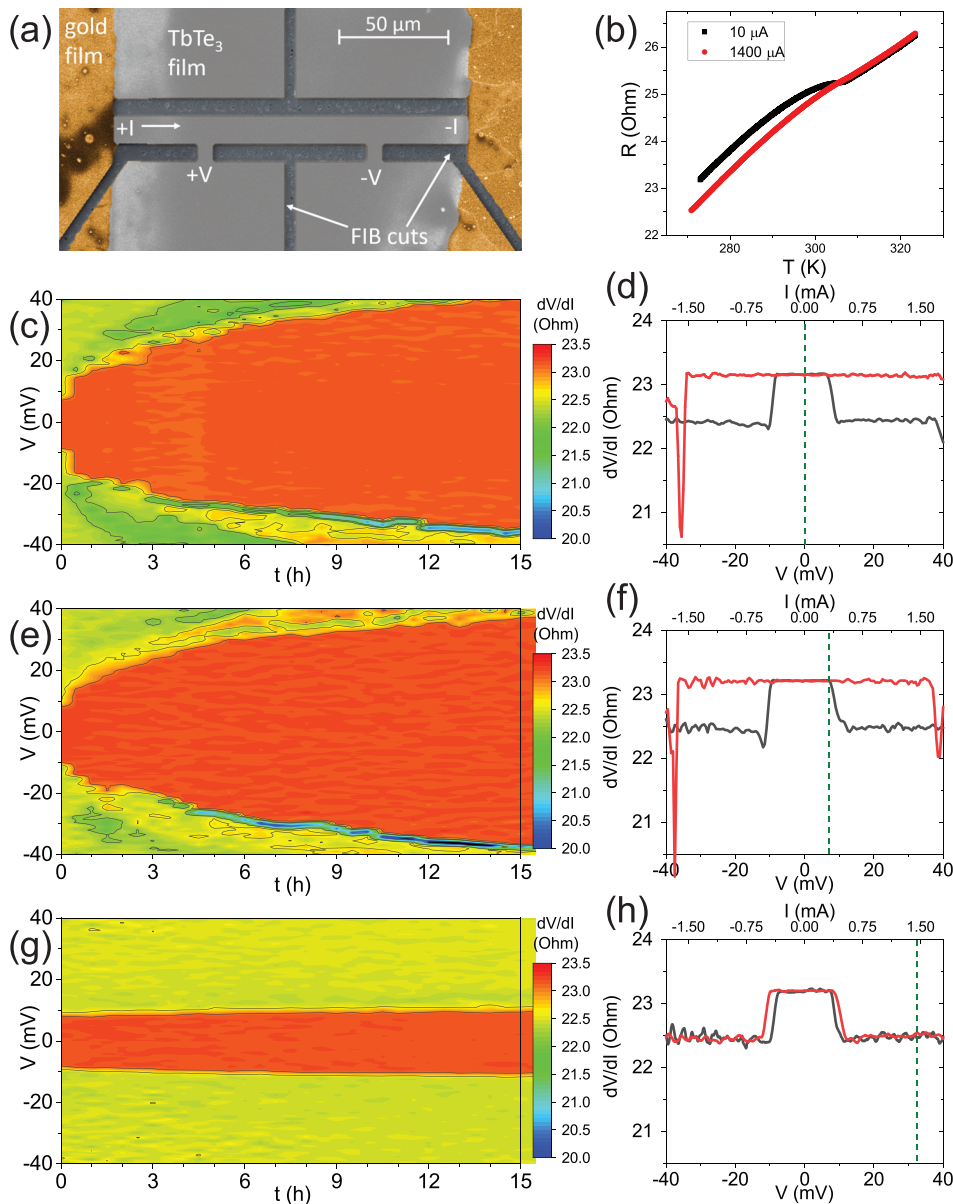


**FIG. 1.** (a) SEM image of structure 1. (b) Temperature dependencies of resistance,  $R(T)$ , in ZEFC (black curves) and EFC (red curves) regimes for structure 1. (c), (e), and (g) Three-dimensional plots of time evolution of differential IVs under exposition of  $\text{TbTe}_3$  (structure 1) at  $T=270\text{ K}$  during 15 h at current 0 (c), 0.3 (e), and 1.4 mA (g). The threshold current for CDW depinning at  $t=0$  is 0.38 mA. (d), (f), and (h) Corresponding initial and final differential IVs. Green lines indicate exposition current  $I_{\text{exp}}$ .  $I$  and  $V$  are converted one into another using the zero-bias relation between the current and voltage.

frequency (rf) irradiation; the most widely studied effect is synchronization of the CDW motion with the external electric field, known also as the interference effect, mode locking, or the Shapiro steps.<sup>2</sup> In the present study, we have observed and compared Shapiro step structures in the ZEFC configuration for structure 1 at  $T=270\text{ K}$  at different exposition times. Figure 3 shows differential IVs under the application of an rf electric field with frequency 20 MHz for exposition time  $t=0\text{ h}$  (black curve),  $t=1.5\text{ h}$  (red curve), and  $t=7\text{ h}$  (green curve). The Shapiro step structure has been observed in all cases.

One can note that the Shapiro step structure is much more developed at  $t_{\text{exp}}=7\text{ h}$  when  $E_t$  has increased significantly. One can evaluate the CDW current,  $\Delta I_{\text{CDW}}$ , from the distance between neighboring Shapiro steps. From Fig. 3, there is no appreciable difference  $\Delta I_{\text{CDW}}$

between different times of exposition. Indeed, there is no change in the sample resistance in the static state of the CDW with time. Similarly, the resistance in the sliding state at maximum of the applied current is the same independently on exposition time [see Figs. 2(c) and 2(d)]. The CDW current is calculated from two contributions to the total electric current,  $I_{\text{total}}$ : normal electrons and collective CDW transport such as  $I_{\text{CDW}} = I_{\text{total}}(1 - \frac{R_N}{R_{\text{total}}})$ , where  $R_{\text{total}}$  is the total resistance and  $R_N$  is the normal carrier resistance, both are determined from direct IV curves. One may conclude that there is no change in the magnitude of the CDW current at long exposition time. The more remarkable effect when samples are electric field cooled with a current less than  $I_t$  is the improvement of the Shapiro step structure, which manifests the better CDW coherency in the CDW motion state.



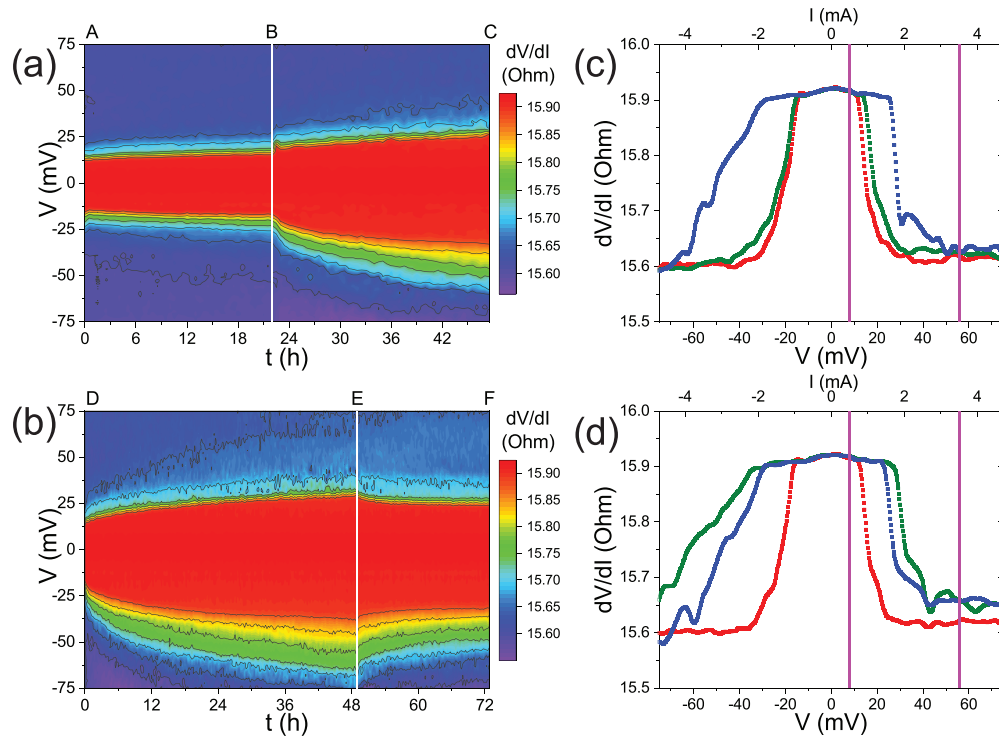


**FIG. 2.** (a) Three-dimensional plots of time evolution of differential IVs under exposition of TbTe<sub>3</sub> (structure 2) at  $T = 280$  K when EFC with an exposition current  $I_{\text{exp}} = 3.5$  mA  $> I_t$  during 22 h (between point A and point B) then after point B at  $I_{\text{exp}} = 0.5$  mA  $< I_t$  26 h until point C; (b) is the same as in (a) but during the time corresponding to the interval D–E, the exposition current was  $I_{\text{exp}} = 0.5$  and in the time interval E–F at current  $I_{\text{exp}} = 3.5$  mA. Panels (c) and (d) show differential IVs at points A (red), B (green), and C (blue) in (c) and at points D (red), E (green), and F (blue) in (d). Pink lines indicate the exposition current.  $I$  and  $V$  are converted one into another using the zero-bias relation between the current and voltage.

After having been cooled through  $T_{CDW1}$  without an applied current or with a small current and kept it at  $T_{\text{exp}}$ , we have found that the threshold field  $E_t$  for depinning the CDW increases exponentially  $E_t(t) \sim (1 - \exp(-t/\tau))$  with a characteristic time  $\tau$  temperature

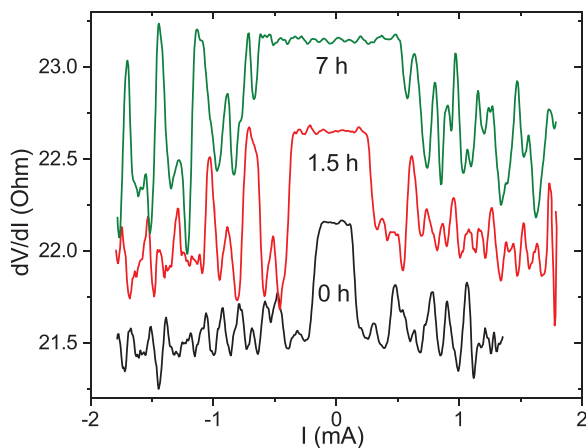


**FIG. 3.** (a) Differential current–voltage characteristics of TbTe<sub>3</sub> (structure 1) cooled without an electric field (ZEFC) down to  $T = 270$  K under the application of an rf electric field with a frequency 20 MHz for  $t_{\text{exp}} = 0$  (black curve),  $t_{\text{exp}} = 1.5$  (red curve), and  $t_{\text{exp}} = 7$  h (green curve). The curves are shifted for clarity.

dependent, typically 40 min at 320 K and  $10^3$  min at 240 K. However, the measurement of the threshold is only used to probe the CDW ground state. In the case of weak pinning randomly distributed impurities, each impurity is too weak to pin the CDW phase, but the CDW can be pinned by the fluctuations of the number of impurities in a large volume, it results that in a single domain, an average well defined phase less than  $\pi$ . So, the sample consists of independent domains. In a single domain with a single phase, the equation of motion of the rigid CDW corresponds to an harmonic damped oscillator. The differential resistance in the case of current mode measurement has an infinite negative value at  $E_t$ .<sup>13</sup> As any sample is made up of many domains, each one with its own  $E_t$ , the divergence at threshold is suppressed. The changes in the shape of  $dV/dI(V)$  characteristics in Figs. 1(d) and 1(f) clearly show this negative jump at  $E_t$  at the end of the relaxation process, indicating that the CDW ground state consists of a single or a very few domains with a constant phase  $\phi$ . Similarly, the improvement of the Shapiro step structure shown in Fig. 3 indicates a better order in the sliding state. But why the threshold electric field for the CDW sliding is much higher in the equilibrium ground state compared with the non-equilibrium one?

One can assume that during the time at which the system is kept at a fixed temperature below  $T_{CDW1}$ , the CDW is reorganized and a new macrostructure develops. The facts that the sample resistance and the magnitude of the Peierls transition temperature do not change during the exposition are indications that nothing changes at the

macroscopic level. Because of the very weak orthorhombicity, one can expect the appearance of some kind of ordering in the transverse to the CDW1 direction, namely, along the  $a$ -axis.

One may also think to the breakdown of the collective pinning and the crossover between weak pinning and strong pinning on some well-ordered structures. The CDW distortion is described by long and large Te-Te bonds in the Te plane. It was also thought as formed of oligomeric fragments of  $(\text{Te}_x)^{2-}$ , typically trimers and tetramers.<sup>14,15</sup> Although the CDW was considered as uniform, the presence of discommensuration was not ruled out.<sup>16</sup> A discommensuration network, which will need time to become well-ordered, may act as strong pinning centers. Similarly to the peak effect in twinned superconductors,<sup>10</sup> trimers in  $\text{RTE}_3$  crystals can also play a role. The effect of the applied current on the charged  $(\text{Te}_x)^{2-}$  oligomeric fragments needs to be more investigated. However, following the model of depinning by the lattice in a strong coupling pinning,<sup>19</sup> in which the modulation function is not sinusoidal but discontinuous, the polarization of the Te-Te bonds with different lengths may modify the local electric field and, therefore, the depinning field.

The very astonishing effect is the time relaxation at  $T_{\text{exp}}$  when the sample is EFC with a current higher than the threshold one; the out of equilibrium CDW ground state is frozen [Fig. 1(g)] and even if relaxation occurs, the time effect would be tremendously long. In the context of definition of a glass transition (when time evolution exceeds the reasonable time of an experiment), one can say, that the ground state is in a glass state, which anchors the weak pinning centers configuration since  $E_t$  is minimal. However, the current that induces this glass state is higher than  $I_t$ . As soon as this current is reduced below  $I_t$ , the relaxation process is resumed [Fig. 2(a)]. On the contrary, when  $I$  is increased above  $I_t$  and when the CDW equilibrium has nearly been reached, there is only a weak effect.

High resolution x-ray diffraction is needed to detect any change in the  $Q$  distortion vector on time as well as any change in the rocking curves of the satellites. The line shape of CDW satellites has been determined for pinned CDW:<sup>17</sup> the power law behavior of the CDW Bragg peaks can reveal a Bragg glass behavior.<sup>18</sup>

In conclusion, we have shown that the CDW ground state of  $\text{TbTe}_3$  when the sample is kept at a given temperature below the Peierls transition temperature evolves toward an equilibrium state with a nearly uniform phase in macroscopic volume. When cooled under an electric field higher than the threshold value for the CDW

sliding at the given temperature, the CDW ground state is a frozen glass state, which can be destabilized only by reducing the electric field below the threshold value. It is worth noting that the characteristic time for relaxation toward equilibrium depends exponentially on temperature. This means that the equilibrium ground state may never be reached at low temperatures.

The authors acknowledge P. Qu  merais and O. Cepas for useful discussions. This work has been supported by the State Assignment IRE RAS.

## DATA AVAILABILITY

The data that support the findings of this study are available within the article.

## REFERENCES

- <sup>1</sup>L. P. Gor'kov and G. Gr  ner, in *Charge Density Waves in Solids, Modern Problems in Condensed Matter Sciences* (North-Holland, Amsterdam, MA, 1986), Vol. 25.
- <sup>2</sup>P. Monceau, *Adv. Phys.* **61**, 325 (2012).
- <sup>3</sup>H. Fr  hlich, *Pro. R. Soc. London, Ser. A* **223**, 296 (1954).
- <sup>4</sup>P. B. Littlewood and R. Rammal, *Phys. Rev. B* **38**, 2675 (1988).
- <sup>5</sup>K. Biljakovi  , J. C. Lasjaunias, P. Monceau, and F. Levy, *Phys. Rev. Lett.* **67**, 1902 (1991).
- <sup>6</sup>L. Mihaly and G. X. Tessema, *Phys. Rev. B* **33**, 5858 (1986).
- <sup>7</sup>A. V. Frolov, A. P. Orlov, A. A. Sinchenko, and P. Monceau, *JETP Lett.* **109**, 203 (2019).
- <sup>8</sup>A. V. Frolov, A. P. Orlov, A. Hadj-Azzem, P. Lejay, A. A. Sinchenko, and P. Monceau, *Phys. Rev. B* **101**, 155144 (2020).
- <sup>9</sup>A. I. Larkin and Y. N. Ovchinnikov, *J. Low Temp. Phys.* **34**, 409 (1979).
- <sup>10</sup>A. I. Larkin, M. C. Marchetti, and V. M. Vinokur, *Phys. Rev. Lett.* **75**, 2992 (1995).
- <sup>11</sup>A. A. Sinchenko, P. Lejay, and P. Monceau, *Phys. Rev. B* **85**, 241104(R) (2012).
- <sup>12</sup>A. A. Sinchenko, P. Lejay, O. Leynaud, and P. Monceau, *Solid State Commun.* **188**, 67 (2014).
- <sup>13</sup>P. Monceau, J. Richard, and M. Renard, *Phys. Rev. B* **25**, 931 (1982).
- <sup>14</sup>D. Malliakas and M. G. Kanatzidis, *J. Am. Chem. Soc.* **128**, 12612 (2006).
- <sup>15</sup>H. J. Kim, C. D. Malliakas, A. T. Tomi  , S. H. Tessmer, M. G. Kanatzidis, and S. J. L. Billinge, *Phys. Rev. Lett.* **96**, 226401 (2006).
- <sup>16</sup>A. Tomic, Z. Rak, J. P. Veazey, C. D. Malliakas, S. D. Mahanti, M. G. Kanatzidis, and S. H. Tessmer, *Phys. Rev. B* **79**, 085422 (2009).
- <sup>17</sup>A. Rosso and T. Giamarchi, *Phys. Rev. B* **70**, 224204 (2004).
- <sup>18</sup>T. Giamarchi and P. Le Doussal, *Phys. Rev. B* **52**, 1242 (1995).
- <sup>19</sup>P. Qu  merais, *Europhys. Lett.* **117**, 57004 (2017).